Annual Reviews
www.annualreviews.org/aronline

Copyright 1973. All rights reserved

MODE OF STRAIN RELEASE ASSOCIATED WITH MAJOR EARTHQUAKES IN JAPAN

* 10009

Hiroo Kanamori
Earthquake Research Institute, Tokyo University, Tokyo, Japan

Annu. Rev. Earth. Planet. Sci. 1973.1:213-239. Downloaded from arjournals.annualreviews.org
by CALIFORNIA INSTITUTE OF TECHNOLOGY on 09/13/05. For personal use only.

INTRODUCTION

It is now widely accepted that most shallow earthquakes are caused by a sudden release of tectonic stress, and therefore strain, in the form of faulting (56, Chap. 14). The elastic rebound theory explains remarkably well the overall nature of major earthquakes. However, it is now evident that the strain release by actual earthquakes takes place in a variety of ways. For example, some earthquakes are reported to have been preceded by significant premonitory crustal deformations with or without foreshocks. Most major earthquakes are followed by aftershocks and, in some cases, by creep-like postseismic deformations. This variety obviously results from the difference in the nature of the crust and the stress field in the respective epicentral area. Thus, detailed study on the mode of the strain release for individual earthquakes is important for understanding the physics of earthquakes and for predicting the mode of occurrence of future major earthquakes. The latter problem is of course very important for designing a practical method of earthquake prediction.

The crustal deformation represents the low frequency spectrum of the strain release, and seismic waves represent the high frequency spectrum. To understand better the mode of the strain release, it is important to study it over a wide frequency range, from geodetic to seismic. From this point of view, this paper discusses the mode of strain release in several major earthquakes in Japan for which both geodetic and seismic data are available, and we will focus our attention on the relation between the geodetic slip and the seismic slip. Figure 1 shows the locations of the earthquakes discussed in this paper. We do not intend to make an exhaustive review of the literature on the subject that can be referred to (19, 21, 36, 39, 50, 63, 71).

SUMMARY OF RESULTS ON EARTHQUAKES

Tottori Earthquake of 1943

This earthquake ($M = 7.4$) occurred on September 10, 1943 on the Japan Sea side of Honshu island, and detailed data on the fault plane solution (17), aftershock

Annual Reviews
www.annualreviews.org/aronline

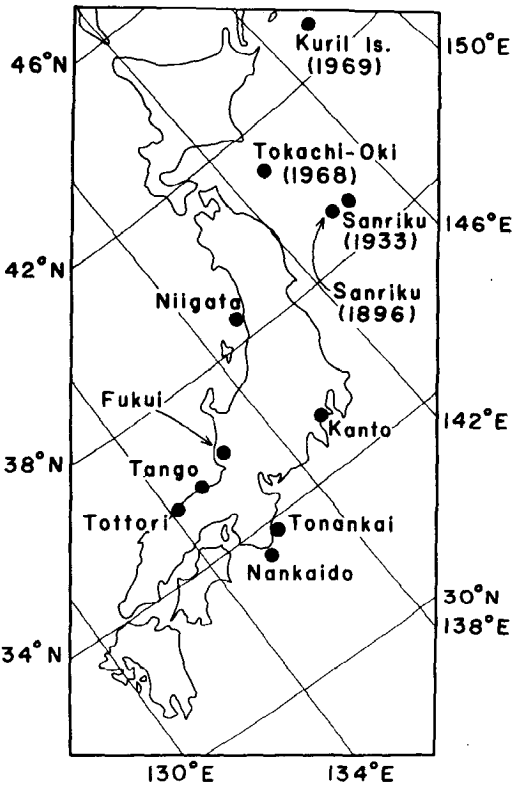

Figure 1 Location of earthquakes.

distribution (55), triangulation (57), and various field observations (66) are available. The triangulation data can be interpreted in terms of a nearly vertical right-lateral fault with a surface offset of 2.5 m (Figure 2a). The length and the strike of the fault can be estimated to be ~33 km and N80°E respectively. The maximum upheaval amounts to 70 cm and the maximum subsidence is 40 cm. However, the vertical displacement is, on the whole, much smaller than the horizontal displacement. The aftershock distribution and the first motion data are consistent with the fault geometry suggested by the triangulation data (Figure 2b, c).

The seismic slip associated with this earthquake has been determined on the basis of a low magnification seismogram recorded at Abuyama Seismological Observatory, whose epicentral distance is only 140 km (26). Comparison of the

Annu. Rev. Earth. Planet. Sci. 1973.1:213-239. Downloaded from arjournals.annualreviews.org
by CALIFORNIA INSTITUTE OF TECHNOLOGY on 09/13/05. For personal use only.

Annu. Rev. Earth. Planet. Sci. 1973.1:213-239. Downloaded from arjournals.annualreviews.org
by CALIFORNIA INSTITUTE OF TECHNOLOGY on 09/13/05. For personal use only.

Annual Reviews
www.annualreviews.org/aronline

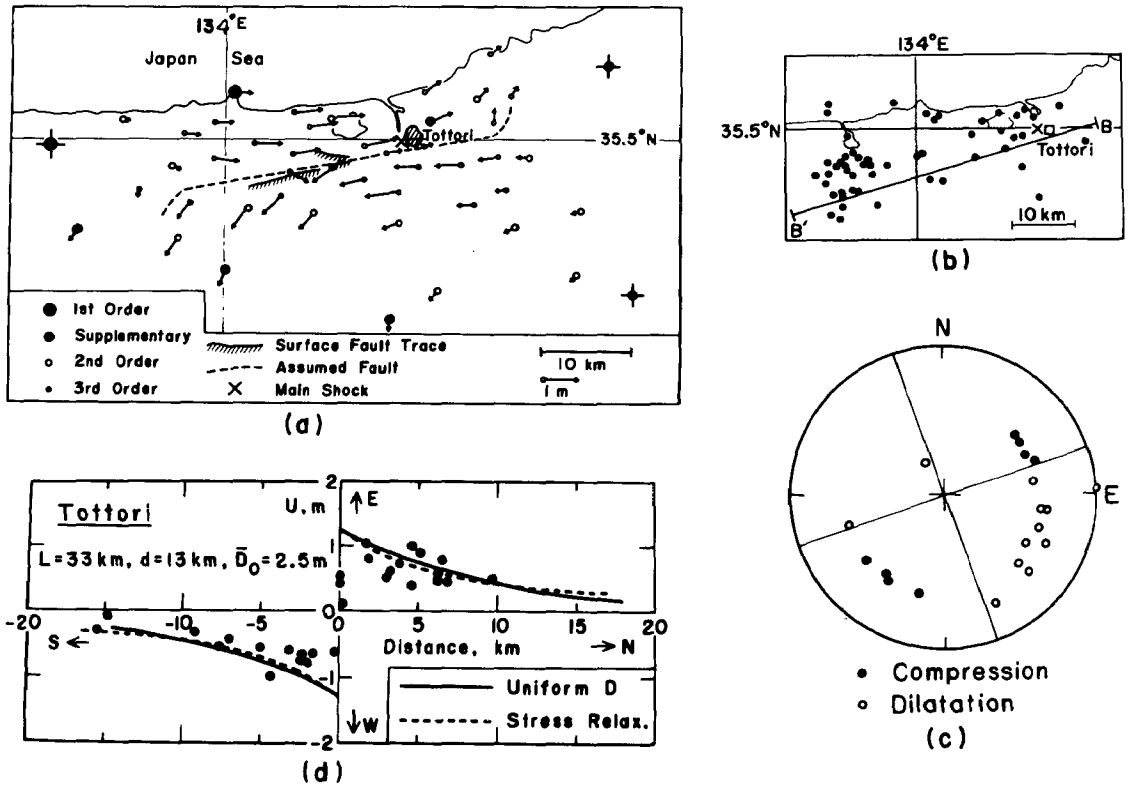

Figure 2 (*a*) Displacement of triangulation points (57), (*b*) aftershocks (55), (*c*) *P*-wave first motion (equal-area projection of the lower half of the focal sphere) (17), and (*d*) displacement parallel to the fault strike (26) of the Tottori earthquake.

Annual Reviews
www.annualreviews.org/aronline

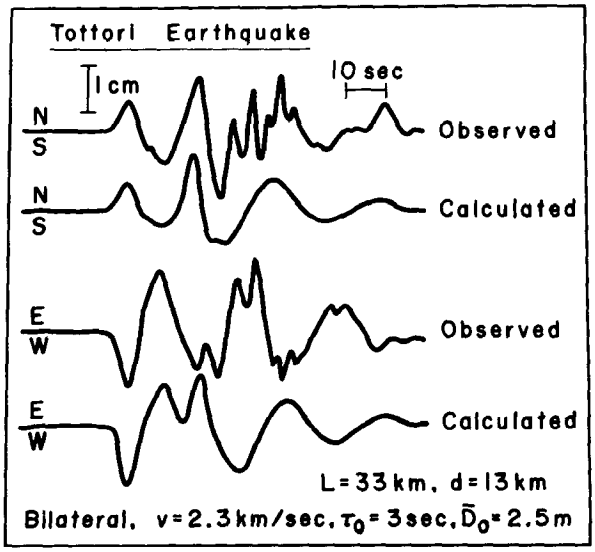

Figure 3 Observed and synthetic seismograms at $\Delta = 140$ km. Seismograph constants are: $T_0 \approx 25$ sec; $\varepsilon \approx 1.8$; $V = 1.2$. L: fault length; d: fault width; v: rupture velocity; τ_0: rise time of the slip dislocation; $\bar{D}_0$: average dislocation (for details, see 26).

seismogram with the synthetic ones calculated by the De Hoop-Haskell method for various fault parameters led to the following results (fault length is assumed to be 33 km) (Figure 3): fault depth, 13 km; average dislocation, 2.5 m; moment, 3.6×10^{26} dyne × cm; stress drop, 83 bars. The seismogram was also used to estimate the stress which accelerated the fault motion. An estimate of 30 to 100 bars, which is about the same order as the stress drop, is obtained for this stress. This result led to the conclusion that most of the stress which had been acting on the fault prior to the earthquake was released at the time of the earthquake.

In comparing the seismic slip with the geodetic data, one problem arises. Figure 2d, which shows the displacement of the triangulation points as a function of distance from the fault, includes two curves computed for two different fault models. The solid curve is for a fault model having a dimension of 33×13 km^2 and a uniform dislocation of 2.5 m. This fault model is in accordance with the model derived from the seismic data. The dotted curve is for a fault model having a dislocation that decays with depth according to Knopoff's (32) stress relaxation model. The dislocation at the surface is 2.5 m, the depth-average dislocation being 2 m. The two models fit the data equally well; in other words, the geodetic data cannot resolve the slip at depths. We may conclude, however, that the seismic slip is in approximate agreement with the geodetic slip.

At the time of the Tottori earthquake, two surface faults (Shikano and Yoshioka) appeared (66). On the basis of the topographical features, Matsuda (35)

Annu. Rev. Earth. Planet. Sci. 1973.1:213-239. Downloaded from arjournals.annualreviews.org
by CALIFORNIA INSTITUTE OF TECHNOLOGY on 09/13/05. For personal use only.

Annual Reviews
www.annualreviews.org/aronline

suggests that the rate of the right-lateral displacement along these faults is $\lesssim 3\,\text{m}/10^4$ years and that there is no evidence of a significant slip during the several thousand years preceding the earthquake.

From the results presented above, it may be concluded that the Tottori earthquake represents a nearly complete and instantaneous release of the tectonic stress which had slowly built up, over a period of about 10^4 years, to ~ 100 bars. This mode of strain release is what might be expected of a purely elastic rebound in which the stored strain energy is released instantaneously following a brittle fracture.

Annu. Rev. Earth. Planet. Sci. 1973.1:213-239. Downloaded from arjournals.annualreviews.org
by CALIFORNIA INSTITUTE OF TECHNOLOGY on 09/13/05. For personal use only.

Fukui Earthquake of 1948

This earthquake ($M = 7.3$) occurred on June 28, 1948 in the central part of Honshu island bordering the Japan Sea. Although no surface fault offset was found after the earthquake, several fissures arranged *en échelon* in a zone striking N10°W to N20°W and the displacement of the triangulation points found by postseismic resurveys clearly suggest the existence of a buried left-lateral fault parallel to the fissure zone (45, 49) (see Figure 4). A thick alluvial cover in the epicentral area probably smeared out the offset in the bedrock. Figure 5 shows the horizontal displacement as a function of distance from the fault, which suggests an offset of ~ 2 m. The epicenters of the aftershocks are scattered over a region extending a distance of ~ 30 km (54), and most aftershocks are shallower than 13 km. The mainshock is located approximately at the center of the aftershock area. The *P*-wave first motion data suggest a vertical strike-slip fault striking either N10°W or N80°E (17) (Figure 4). Combining all these data, we may assume the fault parameters as follows: fault area, 30 km (length) × 13 km (width in depth direction); strike, N10°W to N20°W; dip, $\sim 90°$; offset, ~ 2 m. Because the epicenter of the mainshock is located slightly east of the assumed fault axis and the aftershocks are more densely distributed to the east of the fault than to the west, it is possible that the fault plane is not completely vertical but dips steeply to the east. The triangulation and the first motion data are not complete enough for a precise determination of the dip angle, and it is therefore subject to some uncertainty. Records of a low magnification and long period seismograph obtained at Abuyama Observatory, located at a distance of ~ 155 km, were used to determine the seismic slip. Synthetic seismograms were computed for various fault models, in much the same way as for the Tottori earthquake, and were compared with the observed seismograms to obtain appropriate fault parameters (Figure 6). Because the De Hoop-Haskell method applies only to a homogeneous medium the comparison should be made only for body waves. As shown in Figure 6, the observed seismograms clearly show that this earthquake represents a multiple shock (33, 51). The first shock is followed, after ~ 9 sec, by the second shock, which is about four times as large. Since the spatial relation between the first and the second shocks could not be determined, detailed features of the rupturing process are unknown. The second event, which obviously represents the major event, can be explained in terms of vertical left-lateral faulting in which the fault area, dislocation, rupture velocity, and rise time are 30×13 km^2, 2 m, 2.3 km/sec, and

Annual Reviews
www.annualreviews.org/aronline

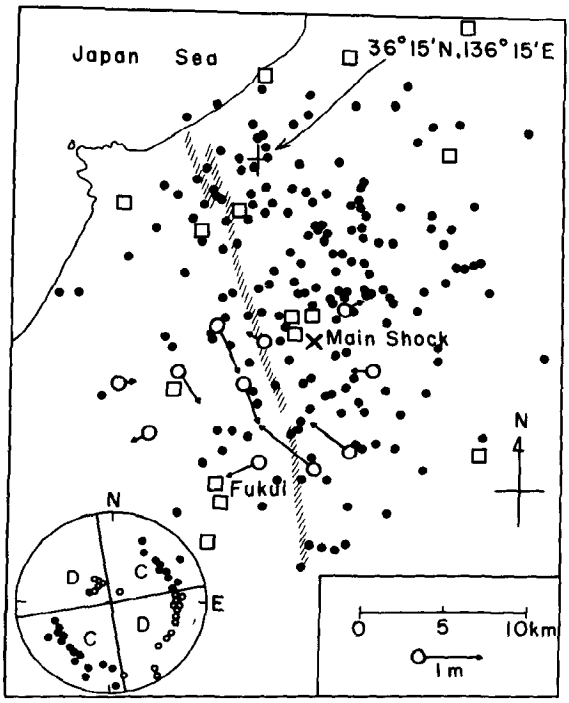

Figure 4 Displacement of triangulation points (45, 49), aftershocks (July 5–August 2) (54), and the *P*-wave first motion data (17) of the Fukui earthquake. Hatchings indicate the zone of surface fissures (49). Squares show the locations of seismographic stations.

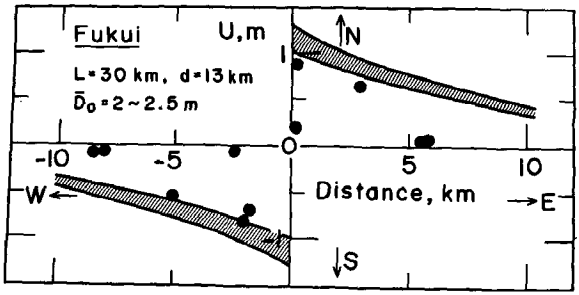

Figure 5 Displacement as a function of distance from the fault. Hatching shows the range calculated for the seismic fault ($\bar{D}_0 = 2$ to 2.5 m).

Annu. Rev. Earth. Planet. Sci. 1973.1:213-239. Downloaded from arjournals.annualreviews.org
by CALIFORNIA INSTITUTE OF TECHNOLOGY on 09/13/05. For personal use only.

Annual Reviews
www.annualreviews.org/aronline

2 sec respectively. To explain the multiple shock feature, the synthetic seismogram $f(t)$ calculated for the above fault model is multiplied by one fourth, displaced backwards by 9 sec, and superposed on $f(t)$. The results are shown in Figure 6. This superposition presupposes a rupture process in which a dislocation of 0.5 m first took place along the entire fault length and, after a lapse of 9 sec, another 2.0 m dislocation occurred. It is not claimed, however, that this superposition provides the sole explanation for the multiple shock feature. The point to be emphasized here is that an overall dislocation of 2 to 2.5 m along the fault length of ~ 30 km is suggested regardless of the detailed rupturing process.

Figure 5 compares the geodetic slip with the seismic slip and indicates that they approximately agree with each other. The seismic moment, the stress drop, and the effective stress determined from the seismic data are 3.3×10^{26} dyne $\times$ cm, 83 bars, and 36 to 120 bars respectively. Thus, the Fukui earthquake shares much the same property as the Tottori earthquake regarding the mode of strain release; that is, the mode of strain release is what is expected of purely elastic rebound.

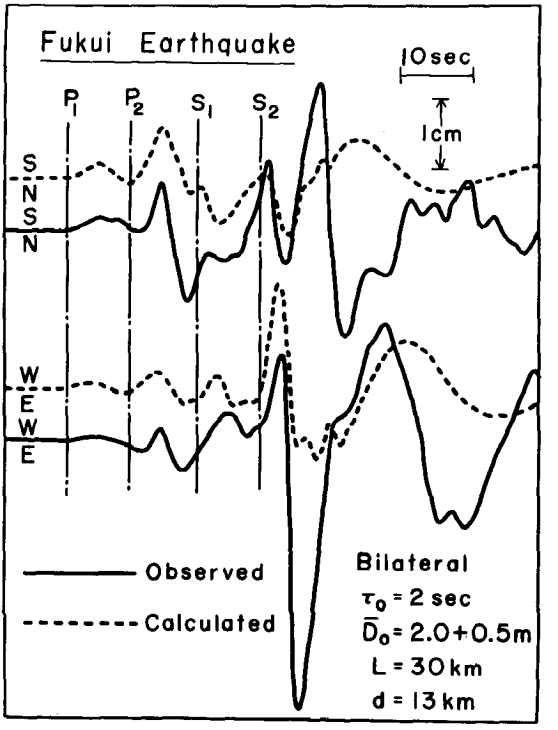

Figure 6 Observed and synthetic seismograms at $\Delta = 155$ km. P_i and S_i indicate the onset of the ith event. For seismograph constants and fault parameters, see caption to Figure 3.

Annu. Rev. Earth. Planet. Sci. 1973.1:213-239. Downloaded from arjournals.annualreviews.org
by CALIFORNIA INSTITUTE OF TECHNOLOGY on 09/13/05. For personal use only.

Annual Reviews
www.annualreviews.org/aronline

Tango Earthquake of 1927

This earthquake ($M = 7.75$) occurred on the Japan Sea side of Honshu island on March 7, 1927 (18). At the time of the earthquake two remarkable seismic faults, the Gomura and the Yamada, appeared as shown in Figure 7 (70). The Gomura fault consists of several parallel cracks arranged *en échelon*. The land to the west of the fault moved southward ~ 2.5 m and was elevated 0.5 m relative to the east. The motion is predominantly left-lateral. The displacement along the Yamada fault is somewhat smaller; the southern side of the fault subsided ~ 0.7 m, and moved ~ 0.7 m westwards, the horizontal motion being right-lateral. These two faults may constitute a system of conjugate faults produced by a single stress system, e.g. east-west compression. Matsuda (35) suggests that there is no evidence of a significant slip along these faults during the several thousand years preceding the earthquake.

The horizontal displacement of the triangulation points associated with this earthquake (34, 63) clearly shows a large left-lateral movement along the Gomura fault (Figures 7 and 8). The maximum dislocation amounts to 2.5 m. This distribution of the horizontal displacement suggests a nearly vertical left-lateral fault which extends over a distance $\geqq 30$ km in the direction N25°W. The aftershocks

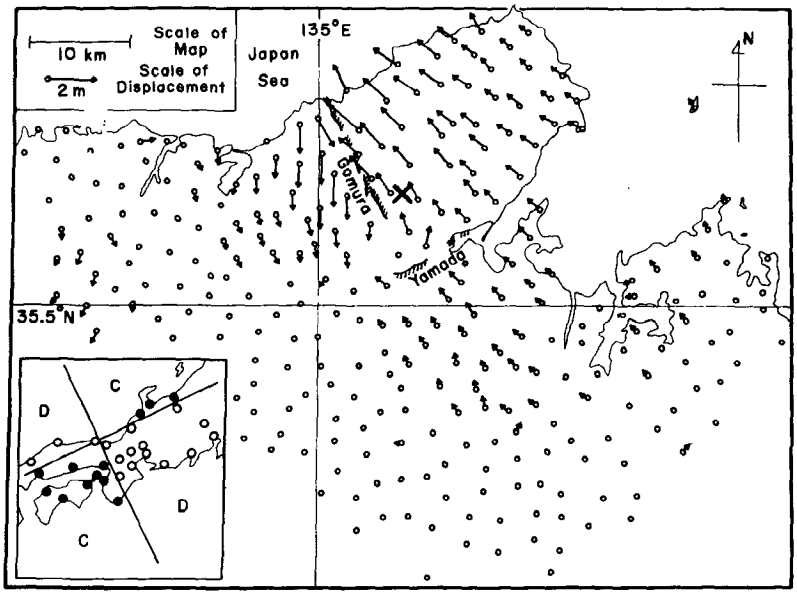

Figure 7 Displacement of triangulation points (34) and the distribution of *P*-wave first motions (16) obtained for the Tango earthquake. The displacements which are less than 30 cm are not shown. The cross mark indicates the mainshock.

Annu. Rev. Earth. Planet. Sci. 1973.1:213-239. Downloaded from arjournals.annualreviews.org
by CALIFORNIA INSTITUTE OF TECHNOLOGY on 09/13/05. For personal use only.

Annual Reviews
www.annualreviews.org/aronline

immediately following the mainshock are distributed more or less along the fault trace (Figure 9). Most aftershocks are shallower than 20 km (48). The distribution of *P*-wave first motions clearly suggests a quadrantal pattern (16) (Figure 7), one nodal line coinciding almost precisely with the fault strike. Kasahara (29) interpreted the triangulation data in terms of a vertical left-lateral fault having a dimension of 30 km (length) × 15 km (width in depth direction) and a surface dislocation of 3 m (see Figure 8).

It is unfortunate that no seismograph record useable for precise determination of the seismic slip is available at short distance; the only seismogram which might be used for this purpose is the one recorded at Tokyo (18) whose epicentral distance is about 430 km. For such a large distance, the synthetic seismograms calculated for homogeneous structure may not be adequate to explain the observed seismogram—in particular, the later part of the seismogram which is affected by various phases caused by the vertical velocity structure. In the present study, an attempt is made to fit only the first half cycle of the *P*-wave. Figure 10 shows a synthetic seismogram for a vertical bilateral fault with a uniform dislocation of 3 m which best fits the observed seismogram among a class of fault models whose length and width are 35 and 13 km respectively. The seismic moment and the stress drop can be estimated as 4.6×10^{26} dyne × cm and 100 bars respectively. This fault model yields horizontal displacements at the surface as shown in Figure 8; the calculated curve fits the triangulation data very well, suggesting that the seismic slip is about the same as the geodetic slip. Although this result is less reliable than those obtained for the Tottori and the Fukui earthquakes because of the large distance, it is unlikely that the two slips differ by a large factor. Thus we may conclude that the mode of the strain release associated with the Tango earthquake is more or less similar to that for the Tottori and the Fukui earthquakes. Most of the accumulated strain was released within a short period of time, about 10 sec.

The postseismic vertical displacement across the Gomura and Yamada faults is well documented (36, 64). Figure 11 shows the relative displacement of the two bench marks located on opposite sides of the fault. It is remarkable that the displacement at the Gomura fault (the major fault of this earthquake) nearly ceased completely within 1 year after the earthquake. The total postseismic displacement is relatively small, about one fiftieth of the coseismic displacement. In contrast, the Yamada fault exhibited a gradual deformation extending over a period of about 20 years. However, the total postseismic displacement is not very large, about 5 cm. Because these bench marks are on alluvium, the postseismic displacements may be accounted for by a compaction of the alluvium. This situation is quite different from that of the 1966 Parkfield earthquake in California, in which a creep-like slip of ~20 cm took place during $1\frac{1}{2}$ years after the earthquake. Because the seismic slip is estimated to be ~10 cm, a substantial amount of displacement, ~10 cm, must have been produced by creep within the bedrock (5, 58).

Determination of the horizontal displacement of the triangulation points was also carried out four times within $1\frac{1}{2}$ years after the Tango earthquake. The

Annu. Rev. Earth. Planet. Sci. 1973.1:213-239. Downloaded from arjournals.annualreviews.org
by CALIFORNIA INSTITUTE OF TECHNOLOGY on 09/13/05. For personal use only.

Annual Reviews
www.annualreviews.org/aronline

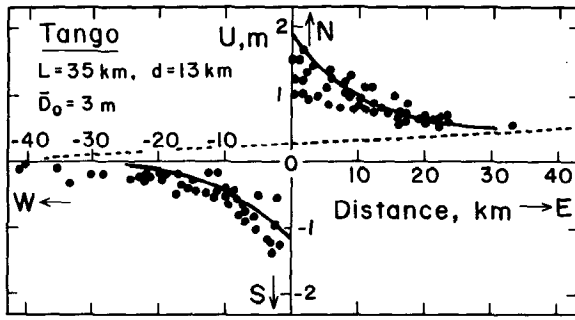

Figure 8 Displacement as a function of distance from the Gomura fault (29). Solid curve shows the displacement for the seismic fault model. The linear trend (dotted line) is corrected according to Kasahara (29).

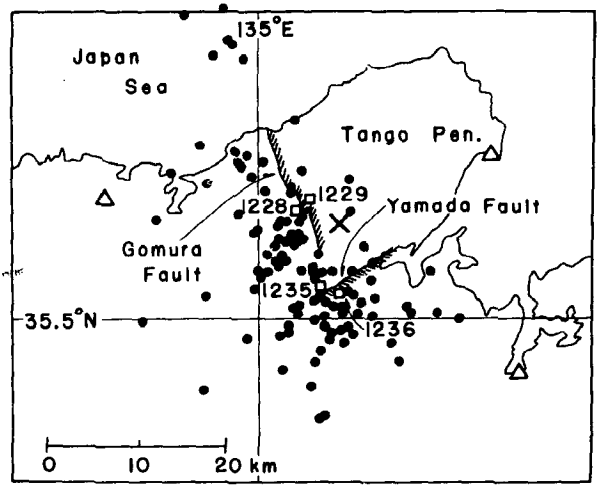

Figure 9 Aftershocks of the Tango earthquake of 1927 (48) for the period from March 12 to March 17. The cross mark indicates the mainshock. The triangles show the location of seismographs. Four leveling bench marks (1228, 1229, 1235, 1236) are shown by squares.

pattern of the horizontal displacement is rather complex and seems to indicate a more or less independent movement of crustal blocks in the epicentral region (64).

Nankaido Earthquake of 1946

This earthquake ($M = 8.2$) occurred on December 20, 1946, about 2 years after the Tonankai earthquake ($M = 8.0$; December 7, 1944). No systematic geodetic surveys were carried out over the entire epicentral area between these two events; therefore, the crustal movement discussed below should be considered to represent a combined effect of these two earthquakes.

Annu. Rev. Earth. Planet. Sci. 1973.1:213-239. Downloaded from arjournals.annualreviews.org
by CALIFORNIA INSTITUTE OF TECHNOLOGY on 09/13/05. For personal use only.

Annual Reviews
www.annualreviews.org/aronline

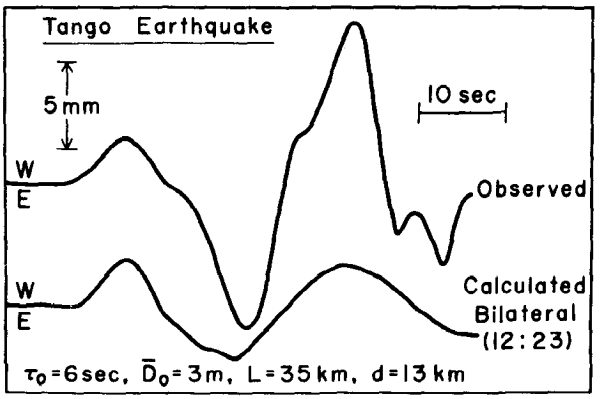

Figure 10 Observed and synthetic seismograms at $\Delta = 430$ km. Seismograph constants are: $T_0 \approx 30$ sec, $\varepsilon \approx 1.6$, $V \approx 1.5$. For fault parameters, see caption to Figure 3.

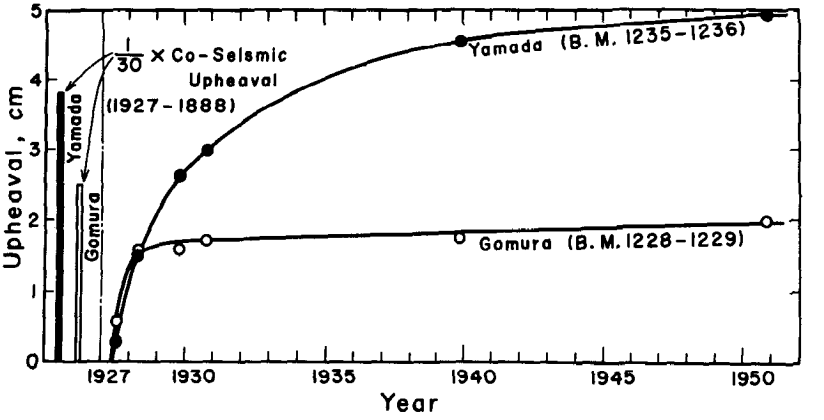

Figure 11 Postseismic change of the relative height between two bench marks across the Gomura and Yamada faults (according to 36, 64, and data obtained by Geographical Survey Institute of Japan). Locations of the bench marks are shown in Figure 9. Coseismic changes are shown for comparison.

The data on the crustal deformation associated with this earthquake are fairly complete for the preseismic, coseismic, and postseismic periods. The vertical movement of the crust was determined on the basis of precise levelings carried out several times both before and after the earthquake (38, 53). Miyabe distinguished the preseismic deformation from the coseismic deformation by assuming that the former is given by a more or less smooth function of time. The results are contoured by Miyabe (38; see also 36). The deformation extends over a large area including Shikoku island and the Kii peninsula (see Figure 12); the general pattern

Annu. Rev. Earth. Planet. Sci. 1973.1:213-239. Downloaded from arjournals.annualreviews.org
by CALIFORNIA INSTITUTE OF TECHNOLOGY on 09/13/05. For personal use only.

Annual Reviews
www.annualreviews.org/aronline

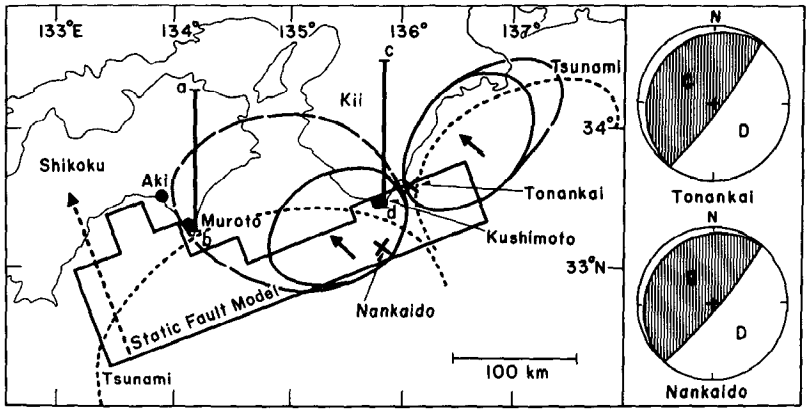

Figure 12 Tonankai and Nankaido earthquakes. The aftershock area 1 day after the mainshock is shown by solid curves and that after 1 month by dashed curves (25). Tsunami source areas are shown by dotted curves (13). The solid polygon shows the projection of the fault plane (9) on the horizontal plane. The solid and dotted arrows show the relative magnitude of the seismic and geodetic slips respectively. The inset shows the mechanism diagrams (stereographic projection) (25).

of the coseismic deformation is characterized by a large uplift at Muroto and Kushimoto and by a subsidence inland. Figure 13 shows the pre- and coseismic deformations along two representative profiles *ab* and *cd* shown in Figure 12. The coseismic deformation is given by a more or less reversed pattern of the preseismic deformation, suggesting that this earthquake is, in a crude sense, represented by a large scale rebound.

The postseismic deformation is known in detail at Muroto where the coseismic upheaval was largest, ~ 1 m. Repeated precise levelings reveal a rapid recovery of the tilt that took place at the time of the earthquake. As shown in the inset of Figure 13a (52, 65), the vertical displacement of Muroto point relative to Aki (see Figure 12), calculated from the tilt measurement, demonstrates a rapid recovery immediately after the earthquake, followed by a more or less uniform subsidence whose rate is approximately the same as that of the preseismic deformation, about -7.5 mm/year. However, as shown in Figure 13, the overall pattern of the postseismic deformation is significantly different from that of the preseismic deformation, indicating that the mode of the recovery is more complicated than that predicted by the simple elastic rebound mechanism. This complexity is also demonstrated by mareographic records at several localities (9, 36). Presumably, several modes of deformation differing in both spatial and temporal characteristics are superposed.

Fitch & Scholz (9) interpreted these data in terms of a rebound on a megathrust beneath southwest Japan. They assumed a location and a strike of the fault and found that a complex thrust fault whose size is about 2.5×10^4 km^2 and whose dislocation varies from 5 to 18 m is required to explain the coseismic vertical deformation (Figures 12 and 14). On the other hand, an earthquake

Annu. Rev. Earth. Planet. Sci. 1973.1:213-239. Downloaded from arjournals.annualreviews.org
by CALIFORNIA INSTITUTE OF TECHNOLOGY on 09/13/05. For personal use only.

Annual Reviews
www.annualreviews.org/aronline

mechanism study (25) suggests that the Nankaido earthquake of 1946 can be explained in terms of a low angle thrust whose size and dislocation are about 10^4 km^2 and 3 m respectively. Figure 12 includes the mechanism diagrams and the aftershock areas.

These results indicate that the seismic slip is significantly smaller, in both magnitude and spatial extent, than the geodetic slip. The aftershock area of the Nankaido earthquake expanded significantly during the period from 1 day to 1 month after the mainshock, as shown in Figure 12 (25, 43, 67). The tsunami source area (13) is even larger than the expanded 1-month aftershock area. Because the aftershock area immediately after the mainshock is likely to represent approximately the extent of the seismic faulting, the above observations all point to a deformation that proceeded gradually and expanded spatially. This type of rebound may be termed a viscoelastic rebound.

The estimate of the geodetic slip itself may be somewhat uncertain. Since the fault assumed by Fitch & Scholz is placed about 100 km off the coast, it predicts that a major deformation would take place beneath the ocean where no data are

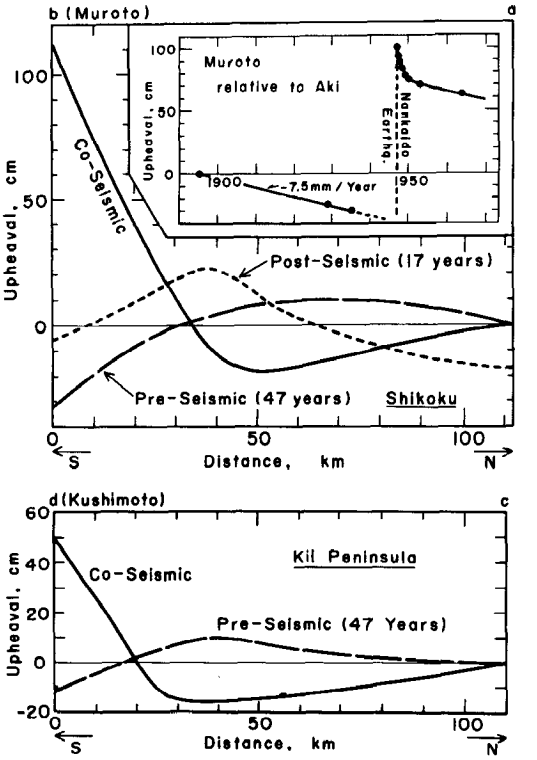

Figure 13 Pre-, co-, and postseismic vertical deformations along the profiles *ab* and *cd* shown in Figure 12 (38, 62). The inset shows the temporal variation of the height of Muroto point relative to Aki (52, 65).

Annu. Rev. Earth. Planet. Sci. 1973.1:213-239. Downloaded from arjournals.annualreviews.org
by CALIFORNIA INSTITUTE OF TECHNOLOGY on 09/13/05. For personal use only.

Annual Reviews
www.annualreviews.org/aronline

available; consequently, the data had to be fit only at the minor trailing end of the predicted curve (Figure 14). Thus, the required maximum dislocation of 18 m seems to depend largely on the assumption of the fault location. Their model predicts a vertical displacement of the ocean bottom as large as 8 m near the western edge of the fault, several times larger than that estimated from the

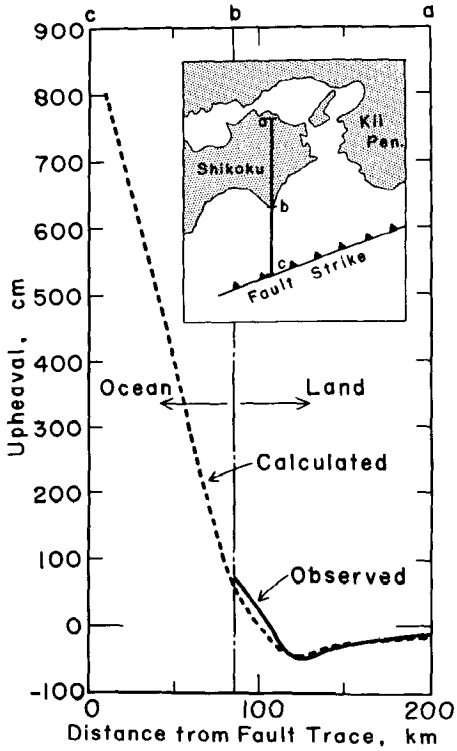

Figure 14 Observed and calculated vertical deformations (9).

tsunami height (13). If the fault model proposed by Fitch & Scholz is correct, this disparity requires a displacement having a time constant longer than several minutes. It is probably also possible to construct a fault model consistent with the tsunami data by adjusting the shape, geometry, and variation of dislocation on the fault plane. These two possibilities are equally likely. The uncertainty in the slip itself, however, does not affect the conclusion that the magnitude of the geodetic slip is significantly larger than that of the seismic slip.

The mode of the deformation revealed above is strikingly different from that suggested for the shallow strike-slip earthquakes such as the Tottori, Fukui, and

Annu. Rev. Earth. Planet. Sci. 1973.1:213-239. Downloaded from arjournals.annualreviews.org
by CALIFORNIA INSTITUTE OF TECHNOLOGY on 09/13/05. For personal use only.

Annual Reviews
www.annualreviews.org/aronline

Tango earthquakes. The large amount of the seismic slip as well as the creep-like recovery suggest some anelasticity operating in the rebound mechanism. Fitch & Scholz (9) also considered an aseismic, and probably anelastic, mechanism to account for the postseismic recovery.

A series of great earthquakes have occurred in the Nankaido region with remarkable temporal regularity; the average repeat time for the last 500 years is about 120 years. Since the product of this repeat time and the rate of the stationary subsidence observed at Muroto (7.5 mm/year) is 90 cm, which is comparable to the coseismic upheaval at Muroto, a coseismic deformation seems to be almost recovered during the subsequent interseismic period. A closer examination reveals the possibility that the postseismic recovery is not complete and that the sequence of great earthquakes in this region resulted in some residual permanent deformation. On the basis of field observations of uplifted marine terraces in the epicentral region, Yoshikawa et al (73) suggested that this mode of land deformation must have continued at least for the past 10^5 years (see also 21, 69, 72). They estimated that about one fifth of the coseismic upheaval at Muroto remained unrecovered during the subsequent interseismic period. This residual upheaval led to a secular upheaval with a rate of about 2 mm/year and to the formation of the sequence of uplifted marine terraces.

Annu. Rev. Earth. Planet. Sci. 1973.1:213-239. Downloaded from arjournals.annualreviews.org
by CALIFORNIA INSTITUTE OF TECHNOLOGY on 09/13/05. For personal use only.

Kanto Earthquake of 1923

This earthquake ($M = 8.2$), which occurred on September 1, 1923 in the neighborhood of Tokyo and Yokohama, is one of the most disastrous earthquakes in history. The coseismic crustal deformation associated with this earthquake is well known (37, 44). The southern tip of the Boso peninsula and the Shonan coast were upheaved 1 to 2 m (see Figure 15); a maximum subsidence of about 1 m took place ~ 50 km inland from the Shonan coast. According to Muto (44), the horizontal displacement is largest in the Boso peninsula; it amounts to 4 to 5 m toward the southeast (see also 56). Recently Ando (6) interpreted these data in terms of a static dislocation model. In this model, the fault plane, 130×65 km^2 in area, dips 45° towards N45°E (Figure 15). A right-lateral displacement of 6 m together with a reverse dip-slip displacement of 2 m are required to explain the observed crustal deformation. Figure 16, which shows two representative profiles along *ab* and *cd* shown in Figure 15, demonstrates the fit between the observed and calculated vertical displacements.

An earthquake mechanism study (22) suggests that the seismic fault plane of this earthquake has a strike of N70°W and a dip of 34° to the northeast (Figure 15). The auxiliary plane strikes N35°E and dips 80° to the southeast; the fault motion is right-lateral reverse. If the size of the fault plane is assumed to be 70×130 km^2, in approximate agreement with the 1-day aftershock area, the average seismic dislocation can be estimated as 2.1 m (Figure 15). These results show that the fault geometry determined by the geodetic data is in approximate agreement with that determined by the seismological data. However, the geodetic slip, ~ 7 m, is significantly larger than the seismic slip of 2 m. This situation is similar to that of the Nankaido earthquake.

Annual Reviews
www.annualreviews.org/aronline

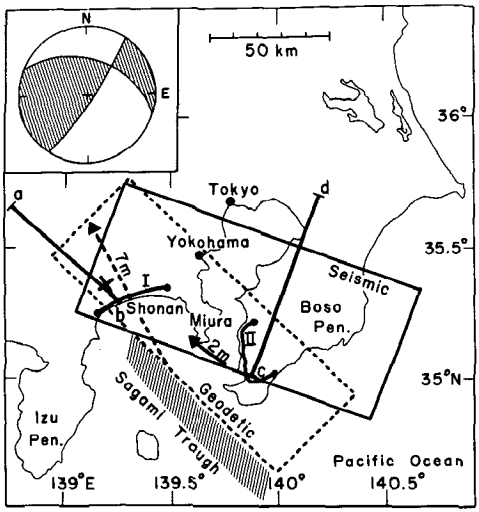

Figure 15 The seismic and geodetic faults of the Kanto earthquake (6, 22). The solid and dotted arrows indicate the seismic and geodetic slips respectively. The epicenter of the mainshock is shown by cross mark. The inset shows the mechanism diagram (stereographic projection). Compression field is hatched.

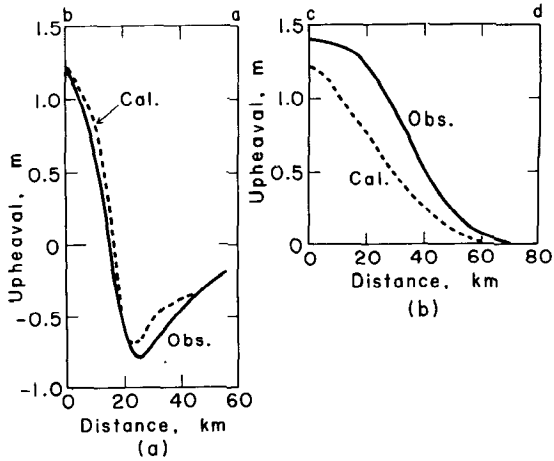

Figure 16 Observed and calculated vertical deformations (6) along the profiles *ab* and *cd* shown in Figure 15.

Annu. Rev. Earth. Planet. Sci. 1973.1:213-239. Downloaded from arjournals.annualreviews.org
by CALIFORNIA INSTITUTE OF TECHNOLOGY on 09/13/05. For personal use only.

Annual Reviews
www.annualreviews.org/aronline

The postseismic deformation has been measured by repeated precise levelings (11). Figure 17 demonstrates the change of the average height of the bench marks along two leveling routes: one along the Shonan coast and the other at the tip of the Boso peninsula (see Figure 15). The coseismic upheaval was largest at these places. In this figure the upheaval is measured from the level at a preseismic time: 1896 for the Shonan coast and 1898 for the Boso peninsula. The solid curves show the change with respect to the datum point in Tokyo. Some evidence suggests that the datum point itself has subsided with a rate of about 1 mm/year during the postseismic period (8). If so, the absolute change can be given by the dotted curves in Figure 17. The recovery of the coseismic upheaval is obvious. The rate is

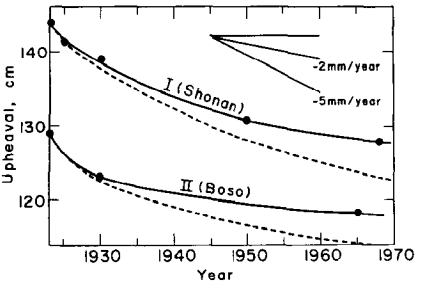

Figure 17 Postseismic change in the height of Boso peninsula (average along the leveling route II shown in Figure 15) and the Shonan coast (average along route I) (11, 36). Solid curves show the change with respect to the datum point in Tokyo. Dotted curves show the absolute change calculated with the assumption that the datum point has subsided with a rate of 1 mm/year.

higher immediately after the earthquake than during the subsequent period. Although this trend is similar to that observed at Muroto (Figure 13), the rate of recovery is significantly lower. The rate of stationary subsidence approaches ~ 2 mm/year.

Sugimura & Naruse (60, 61; see also 68) found a close correlation between the coseismic upheaval at the time of the 1923 Kanto earthquake and the height of Holocene marine terraces observed at several localities along the coast of south Kanto. They suggested that the coseismic upheaval associated with major earthquakes in the past was not recovered completely during the subsequent interseismic period and that the accumulation of the residual upheaval led to a succession of marine terraces. The uplifting of this mode has continued at least for the last 7000 years, and the average rate during this period is ~ 3.3 mm/year. They found that the ratio of the upheaval during the last 7000 years to the coseismic upheaval of the 1923 event is, on the average, 11.

If we let τ, h, r, and H represent the repeat time of major earthquakes, the coseismic upheaval, the recovery rate averaged over the interseismic period, and

Annu. Rev. Earth. Planet. Sci. 1973.1:213-239. Downloaded from arjournals.annualreviews.org
by CALIFORNIA INSTITUTE OF TECHNOLOGY on 09/13/05. For personal use only.

Annual Reviews
www.annualreviews.org/aronline

the secular upheaval during the period of T respectively, we can easily derive $\tau = T/(H/h + rT/h)$. If we take, as representative values, $r = 2$ to 3 mm/year and $h = 130$ cm (from Figure 17), and $H/h = 11$, and $T = 7000$ years (from 60), we have $\tau = 260$ to 320 years. The fractional residual upheaval for each event becomes $(h - r\tau)/h = 0.4$ to 0.5. Sugimura (59) obtained a somewhat shorter repeat time but his estimate is based on the assumption that $(h - r\tau)/h = 0.2$, which is not warranted. These estimates are, of course, very crude owing to the uncertainty in various parameters, particularly the recovery rate. Yet this result seems to indicate that, although the overall pattern of the crustal deformation in the Kanto region is similar to that in the Nankaido region, the repeat rate of major earthquakes and the recovery rate are 2 to 3 times lower in the Kanto region than in the Nankaido region.

The repeat time of major earthquakes in the Kanto region is not known in detail. Imamura (20) considered that only two events in history, one in 818 and the other in 1703, were truly comparable to the 1923 event. In this case the repeat time is from 200 to 900 years, and is much longer than that for the Nankaido region, about 120 years. However, the evaluation of the size of historical earthquakes is inevitably subject to large uncertainty, and some major earthquakes may well have escaped notice.

On the whole, it is concluded that the mode of the strain release associated with the Kanto earthquake of 1923 is more complicated than the simple elastic rebound theory predicts. The geodetic slip which was large compared with the seismic slip, the creep-like recovery immediately after the earthquake, and the residual permanent deformation all suggest a viscoelastic rebound.

Extremely large subsidence with a maximum of 400 m was reported to have taken place in parts of Sagami Bay. The reliability of the data has been much debated (see 56). Reexamination by A. Mogi (40) suggests that such large subsidence can be in error, but a subsidence of some 50 m around the Sagami trough seems significant. Although this value still seems excessive in view of the relatively small tsunamis as well as the displacements on land, it cannot be totally dismissed in view of the viscoelastic nature of the deformation associated with this earthquake; this subsidence, if real, may be related to the origin of the Sagami trough.

Niigata Earthquake of 1964

This earthquake ($M = 7.4$) occurred on June 16, 1964, off the Japan Sea coast of Honshu island. Unlike the Tottori, Fukui, and Tango earthquakes, which occurred on the Japan Sea side and are characterized by a vertical strike-slip faulting, the Niigata earthquake is characterized by a steep dip-slip faulting (3, 4, 15). Fortunately, echo-sounding surveys of the sea bottom topography were carried out in the epicentral area immediately before the earthquake. The echo-sounding surveys were repeated immediately after the earthquake to determine the coseismic vertical displacement (41). The maximum upheaval and subsidence amount to 6 and 4 m respectively, giving a maximum offset of 10 m. The average offset, however, is considerably smaller.

The aftershock area extends over a distance of 80 to 100 km in the direction

Annu. Rev. Earth. Planet. Sci. 1973.1:213-239. Downloaded from arjournals.annualreviews.org
by CALIFORNIA INSTITUTE OF TECHNOLOGY on 09/13/05. For personal use only.

Annual Reviews
www.annualreviews.org/aronline

N20°E. Most aftershocks are shallower than 25 km (31). The mainshock is located at about the center of the aftershock area. The aftershock area coincides approximately with the tsunami source area where the average height of the sea level disturbance is estimated to be ~ 1.5 m (12). Thus, the field studies suggest that the source of the Niigata earthquake can be represented by a bilateral faulting extending over a distance of 80 to 100 km in the direction N20°E to N30°E and to a depth of 20 km or so. Body wave mechanism studies (3, 4, 15) suggest a pure reverse dip-slip fault dipping 60 to 70° towards the west and striking N10°E to N20°E.

The seismic slip has been determined by long period Love waves (3, 4) and by body waves (15) to be 4 to 5 m on a fault plane 20×80 to 100 km^2 in area; this result is in general agreement with that inferred from the field studies. In fact, this agreement was the basis on which Aki (4) substantiated the idea that an earthquake is a release of accumulated strain energy by a rupture. However, quantitative comparison of the seismic results with the results of the field studies is not very straightforward. Crude comparison may be made as follows (1): First, static crustal deformation is computed for the fault model predicted by the seismic results. Then the computed vertical displacement is averaged over the tsunami source area. An average of 1.6 m is obtained in approximate agreement with that inferred from the tsunami data. The echo-sounding results are obtained only along the assumed fault trace. The sense of the displacement, subsidence to the east and upheaval to the west, is consistent with the seismic results. The magnitude of the displacement taken at face value is about twice as large as the seismic results. The distribution, however, is rather jagged, indicating the effect of possible secondary offsets. Thus the displacement, if averaged over a larger area, would become considerably smaller and approach the value predicted by the seismic results. It seems reasonable, therefore, to conclude that the geodetic slip can be slightly larger than the seismic slip, but not by more than a factor of 2.

An islet called Awashima, located about 10 km north of the epicenter, was upheaved by 80 to 160 cm and tilted by 56″ to the west at the time of the earthquake (47). Nakamura et al (47) suggested that a secular tilt similar to that observed at Muroto must have taken place for the last 10^5 years; however, the rate is probably several times less than that at Muroto.

Other Earthquakes

Large earthquakes frequently occur off the Pacific coast of the Japanese islands. Because of inaccessibility to the epicentral area, data on the crustal deformation are lacking or very incomplete for these earthquakes. However, data on tsunamis set off by these earthquakes may provide some information pertaining to the long period spectrum of the source deformation. Unfortunately, the interpretation of tsunami data in terms of crustal deformation at the source is severely hampered by the complex effect of coastal topography on tsunami propagation. Nevertheless, combined use of seismic and tsunami data can reveal, to some extent, a very important difference in the mode of the strain release among these earthquakes. For example, two Sanriku earthquakes, one in 1896 ($M \approx 7.4$ to 7.9) and the

Annu. Rev. Earth. Planet. Sci. 1973.1:213-239. Downloaded from arjournals.annualreviews.org
by CALIFORNIA INSTITUTE OF TECHNOLOGY on 09/13/05. For personal use only.

Annual Reviews
www.annualreviews.org/aronline

other in 1933 ($M = 8.5$), show a striking contrast in the generation of tsunamis and seismic waves. Although the 1896 event is only a moderate earthquake, it generated one of the most devastating tsunamis in history. The 1933 event, on the contrary, is truly a great earthquake, but the tsunami accompanying this earthquake was no larger than that of the 1896 event. Although the instrumental data are very incomplete for the 1896 event, the above difference is irrefutable on the basis of the macroseismic data. This difference is explained in terms of a difference in the mode of the strain release at the source (27). By comparing the height of the sea level disturbance at the tsunami source area estimated by Green's method (14) with the seismic results, Kanamori (27) suggested that the 1896 event requires a time constant $\gtrsim 100$ sec for the source deformation, while the 1933 event may be explained in terms of "instantaneous" dislocation. Thus, the 1933 event seems to represent a purely elastic rebound but the 1896 event, a more or less viscoelastic rebound.

For recent earthquakes, seismological data are more complete and permit a more rigorous discussion. For the 1968 Tokachi-Oki earthquake ($M = 7.9$) and the 1969 Kurile Islands earthquake ($M = 7.8$), the parameters of the seismic faulting are known in detail. Abe (1) computed the deformation of the sea bottom predicted by the seismic fault models and found that the predicted vertical deformation is consistent in both sense and magnitude with the sea level disturbance estimated from the tsunami data obtained along the coast (Figure 18). Although some un-

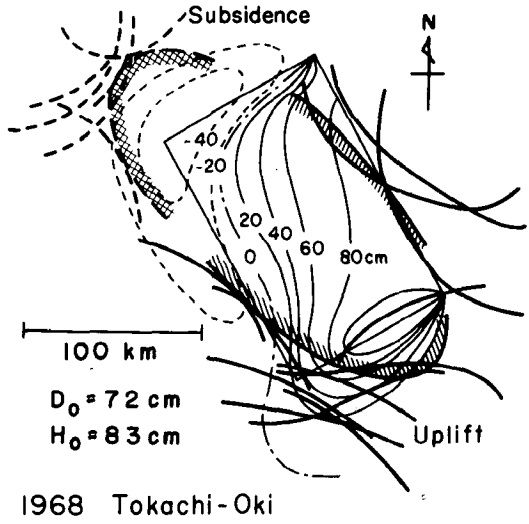

Figure 18 Vertical deformation of the sea bottom predicted by the seismic fault model (thin curves) and the wave front (thick curves) at the tsunami source area of the 1968 Tokachi-Oki earthquake (1). D_0 is the average vertical displacement predicted by the seismic fault and H_0 is the average sea level disturbance at the tsunami source area.

Annu. Rev. Earth. Planet. Sci. 1973.1:213-239. Downloaded from arjournals.annualreviews.org
by CALIFORNIA INSTITUTE OF TECHNOLOGY on 09/13/05. For personal use only.

Annual Reviews
www.annualreviews.org/aronline

certainty is unavoidable in interpreting the tsunami data in terms of the wave height at the source, the above results indicate that the seismic slip does not differ greatly from the geodetic slip. This situation is quite different from that for the Nankaido and the 1896 Sanriku earthquakes where the source deformation responsible for the tsunami generation is of much larger magnitude than that for seismic waves.

CONCLUSIONS

Preceding discussions clearly demonstrate that the mode of the strain release is markedly different among major earthquakes in Japan. For the three shallow strike-slip earthquakes on land (Tottori, Fukui, and Tango) and the Niigata earthquake, the strain release is more or less instantaneous, as the simple elastic rebound theory suggests. A possible explanation is that the fault extends to a depth of only 13 to 20 km where the crustal rocks are brittle enough to cause a sudden fracture. The slow slip rate ($\leqq 3$ m/10^4 years) may contribute to maintaining the brittleness. This situation may be contrasted to that along a part of the San Andreas fault in California, where the slip rate is about two orders of magnitude larger and creep-like slips are taking place.

Among the major earthquakes on the Pacific coast, the Nankaido and the Kanto earthquakes exhibit large aseismic, and probably anelastic, deformations.

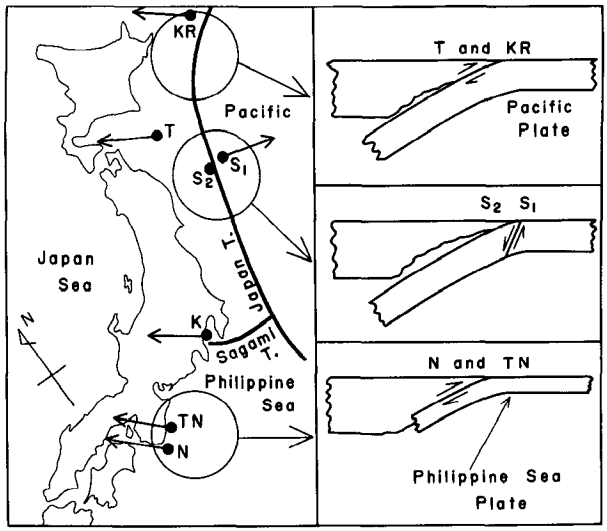

Figure 19 Great earthquakes on the Pacific coast (*KR*: Kuril Islands; *T*: Tokachi-Oki; S_1: Sanriku (1933); S_2: Sanriku (1896); *K*: Kanto; *TN*: Tonankai; *N*: Nankaido), and the mode of lithospheric interaction (23, 25). The arrows show the direction of slip vector of each earthquake (1, 25).

Annu. Rev. Earth. Planet. Sci. 1973.1:213-239. Downloaded from arjournals.annualreviews.org
by CALIFORNIA INSTITUTE OF TECHNOLOGY on 09/13/05. For personal use only.

Annual Reviews
www.annualreviews.org/aronline

This type of deformation cannot be adequately explained in terms of the simple elastic rebound theory. Some viscoelasticity may have to be invoked in the rebound mechanism. The Nankaido earthquake is considered to represent a rebound at the interface between the underthrusting Philippine Sea plate and Honshu island (Figure 19) (9, 25). The underthrusting seems to extend to a depth of 80 km or so (25). The mantle at this depth beneath Honshu island and the Philippine Sea is characterized by abnormally low seismic wave velocity (2, 28). Because low seismic wave velocity is indicative of high temperature, and probably of partial melting, the material at this depth in this region may be more anelastic than that elsewhere. Thus, if the rebound involves the mantle to such depths, it is not surprising that a large amount of anelastic slip accompanies the rebound.

The mode of the rebound associated with the Kanto earthquake is different from that of the Nankaido earthquake. There is, in fact, no obvious evidence for underthrusting of the Philippine Sea plate in the Kanto region. The Kanto earthquake seems to represent a right-lateral slip between the northeastern edge of the Philippine Sea plate and Honshu island. It is possible that this right-lateral motion is affected by the presumably viscoelastic mantle beneath Honshu island and the Philippine Sea plate.

The contrast between the two Sanriku earthquakes has been discussed by Kanamori (27). The 1933 event probably represents a large scale normal faulting in a homogeneous, and probably brittle, oceanic lithosphere, whereas the 1896 event is a manifestation of viscoelastic weak zone formed by the interaction between the oceanic and the continental lithospheres (Figure 19).

The Tokachi-Oki earthquake and the Kurile Islands earthquake can be regarded as "elastic rebound" earthquakes, if the interpretation of the tsunami data is correct. Earthquake mechanism studies (1, 23) suggest that these earthquakes are caused by the underthrusting Pacific plate (Figure 19). This mechanism as it stands is similar to that of the Nankaido earthquake. Then there arises the question as to why the nature of the strain release is different. Provisionally, the following possibility may be suggested as an answer. According to an evolutionary model of earthquakes (23) the Tokachi-Oki and the Kurile Islands earthquakes represent a stage in which the coupling between the oceanic and the continental lithospheres is still large enough to prevent anelastic slip, whereas the Nankaido earthquake represents a stage in which the coupling is once completely weakened, probably by frictional heating. This weakened coupling may be responsible for the aseismic slip.

Interestingly, the coastal marine terraces are most extensively developed in the region where "viscoelastic rebound" earthquakes occurred near the coast (Nankaido and Kanto). It is suggested that the late Quaternary topography of the Japanese islands is affected to a large extent by the mode of the strain release associated with earthquakes (71, 72).

Relation to Earthquake Prediction

Prediction of earthquakes or, more precisely, estimation of likelihood of earthquake occurrence is undoubtedly one of the major goals of seismology. The most direct method of earthquake prediction involves the detection of premonitory phenomena.

Annu. Rev. Earth. Planet. Sci. 1973.1:213-239. Downloaded from arjournals.annualreviews.org
by CALIFORNIA INSTITUTE OF TECHNOLOGY on 09/13/05. For personal use only.

Annual Reviews
www.annualreviews.org/aronline

Because such premonitory phenomena, if any, and the coseismic strain release are both governed by the property of the crust and mantle in the epicentral area, the mode of strain release may provide some inference as to what kind of premonitory phenomenon is to be expected. For example, if the mode of coseismic strain release is more or less elastic, and the faulting does not show any significant anelastic behavior, then anelastic long term premonitory deformation is unlikely to take place. Of course, if some triggering mechanisms such as intrusion of magmas and phase change cause the final fracturing, then they may cause some premonitory deformation just before the earthquake. In fact, for several earthquakes on the Japan Sea coast, premonitory land upheavals are reported to have taken place several minutes to several hours before the earthquake (see Table 1). These results are based on either

Table 1 Earthquakes Preceded by Premonitory Upheaval[a]

					Premonitory deformation	
Earthquake	Date[b]	Latitude (°N)	Longitude (°E)	M	Maximum upheaval (m)	Time before mainshock (hours)
Ajigasawa	Dec. 28, 1793	40.7	140.0	6.9	1 to 2	4
Sado	Dec. 9, 1802	37.8	138.4	6.6	1	5
Hamada	Mar. 14, 1872	34.8	132.0	7.1	2 to 3	0.2
Tango	Mar. 7, 1927	35.6	135.1	7.5	1	2.5

[a]For detailed descriptions, see (19, 21).
[b]Japan time.

descriptions in old literature or interviews with eyewitnesses reporting a retreat of the seawater. On the Japan Sea coast, the maximum tidal variation of the sea level is very small, ~40 cm, so that the retreat of the seawater can be easily recognized. However, none of these upheavals has been observed with instruments, and just a brief description in the original literature has been repeatedly quoted. Objective evaluation of these data seems extremely difficult.

For these "elastic rebound" earthquakes, foreshocks probably represent a more likely premonitory event, although the occurrence of foreshocks strongly depends on the nature of the crust (42), so that such foreshock activity cannot always be expected. The Tottori earthquake of September 10, 1943 was preceded by two relatively large foreshocks ($M \approx 6.1$) in March of the same year. The Tango earthquake of 1927 was preceded by a large earthquake (Tajima earthquake, $M = 6.75$) that occurred on May 23, 1925, ~20 km west of the epicenter of the Tango earthquake.

If the mode of coseismic strain release is more or less viscoelastic, then it would not be surprising if the earthquake with such rebound characteristics is preceded by long term viscoelastic premonitory crustal deformation. For the Kanto and the Nankaido earthquakes such premonitory deformations have been suspected to have taken place. Either tide-gauge record or the result of precise levelings, or both, indicated a reversal in the sense, or a slowdown in the rate, of the crustal deformation several years before the earthquake (10, 19, 65). These results, however,

Annu. Rev. Earth. Planet. Sci. 1973.1:213-239. Downloaded from arjournals.annualreviews.org
by CALIFORNIA INSTITUTE OF TECHNOLOGY on 09/13/05. For personal use only.

Annual Reviews
www.annualreviews.org/aronline

are marginal and confirmation must await future investigations. That some anelastic premonitory deformations take place involving the entire Philippine sea plate has also been suggested on the basis of a causal relation between great earthquakes, earthquake swarm activity, and volcanic activity in a region bordering the Philippine Sea (24, 46). An enhancement of swarm activity and a large scale volcanic eruption in some cases precede the occurrence of great earthquakes by several years, indicating a commencement of a premonitory strain change. Kasahara (30) suggested, on the basis of tilt records obtained at two observatories about 20 km apart, a migration of a strain field in south Kanto with an extremely low velocity, 20 km/year, that indicates some anelastic process.

Relation to Earthquake Engineering

The spectrum of seismic waves at short distance, very important from the point of view of earthquake engineering, strongly depends on the mode of faulting. Previous discussions show that the stress which accelerates the fault motion is significantly different among earthquakes. For example, the Tottori and Fukui earthquakes which represent shallow strike-slip earthquakes on land are characterized by a stress of about 100 bars and a particle velocity of faulting of about 1 m/sec. On the other hand, the stress drops associated with the major earthquakes on the Pacific coast such as the Nankaido and the Kanto earthquakes are around 30 bars (22, 25), which is significantly smaller than that for the earthquakes on land (26) and the Niigata earthquake (4, 15). These earthquakes, however, are characterized by a large fault area. Thus, the shape of the seismic spectrum can be quite different between these two groups of earthquakes. The spectrum of the earthquakes on the Pacific coast may possibly be enhanced at long period, and of those on land at short period. It is emphasized that this difference should be more fully studied in the future in connection with earthquake engineering problems.

Relation to Tsunami

Tsunamis are very disastrous; consequently, establishment of a reliable tsunami warning system is important. Tsunami warning is usually made primarily on the basis of the magnitude of the earthquake. However, tsunamis can be excited by deformations having a time constant of several hundred seconds, while the earthquake magnitude is determined at ~ 10 to 20 sec. Since the spectrum of seismic waves is now known to be quite different among earthquakes, prediction of tsunami potential on the basis of short period data alone can be very hazardous; some earthquakes may have a small earthquake magnitude, yet have a large tsunami potential. The 1896 Sanriku earthquake and the 1946 Aleutian Islands earthquake are examples of such earthquakes, although these probably represent relatively rare events. However, considering the extraordinary damage caused by a single event of this kind (the 1896 event caused 27,122 casualties), we cannot dismiss them simply because they are rare. A warning system based on a wide band spectrum is strongly suggested (7, 27).

The results and conclusions presented in this paper are based mostly on old data, some of which are inevitably incomplete and unreliable. However, the recent

Annu. Rev. Earth. Planet. Sci. 1973.1:213-239. Downloaded from arjournals.annualreviews.org
by CALIFORNIA INSTITUTE OF TECHNOLOGY on 09/13/05. For personal use only.

Annual Reviews
www.annualreviews.org/aronline

development in theory and instrumentation will undoubtedly lead to more refined and reliable results pertaining to the physics of earthquakes. It is hoped that these results will help to reduce the disasters caused by earthquakes as well as help to understand better the tectonic processes taking place in the earth.

ACKNOWLEDGEMENTS

Discussions held with Tokihiko Matsuda, Kazuaki Nakamura, Katsuyuki Abe, and Masataka Ando have been extremely helpful in completing this work. I am much indebted to Kennosuke Okano, Masaji Ichikawa, Naomi Fujita, Takeshi Dambara, and Atushi Okada for some of the material used in this paper. Comments and information provided by Kinjiro Kajiura, Keichi Kasahara, Setumi Miyamura, Kiyoo Mogi, Arata Sugimura, Ietsune Tsubokawa, Kenshiro Tsumura, and Torao Yoshikawa are also gratefully acknowledged. Finally, I thank Tatoko Hirasawa who assisted me throughout this study.

Literature cited

1. Abe, K. 1973. Tsunami and mechanism of great earthquakes. *Phys. Earth Planet. Interiors.* In press
2. Aki, K. 1961. Crustal structure in Japan from the phase velocity of Rayleigh waves, 1. *Bull. Earthquake Res. Inst. Tokyo Univ.* 39:255–83
3. Aki, K. 1966. Generation and propagation of G waves from the Niigata earthquake of June 16, 1964, 1. *Bull. Earthquake Res. Inst. Tokyo Univ.* 44: 23–72
4. Aki, K. 1966. Generation and propagation of G waves from the Niigata earthquake of June 16, 1964, 2. *Bull. Earthquake Res. Inst. Tokyo Univ.* 44: 73–88
5. Allen, C. R., Smith, S. W. 1966. Parkfield earthquakes of June 27–29, Monterey and San Luis Obispo counties, California. Pre-earthquake and post-earthquake surficial displacements. *Bull. Seismol. Soc. Am.* 56:966–67
6. Ando, M. 1971. A fault-origin model of the great Kanto earthquake of 1923 as deduced from geodetic data. *Bull. Earthquake Res. Inst. Tokyo Univ.* 49:19–32
7. Brune, J. N., Engen, G. R. 1969. Excitation of mantle Love waves and definition of mantle wave magnitude. *Bull. Seismol. Soc. Am.* 59:923–33
8. Dambara, T., Hirobe, M. 1964. Vertical movements of Japan during the past 60 years, 1. *J. Geodetic Soc. Jap.* 10:61–70 (in Japanese)
9. Fitch, T. J., Scholz, C. H. 1971. Mechanism of underthrusting in southwest Japan: A model of convergent plate interactions. *J. Geophys. Res.* 76:7260–92
10. Fujita, N. 1971. Tidal observation and earthquake prediction. *Mar. Sci.* 3:562–66 (in Japanese)
11. Geographical Survey Institute of Japan. 1969. Crustal deformation in the Boso and the Miura peninsula. *Rep. Coord. Comm. Earthquake Predict.* 1:25–33 (in Japanese)
12. Hatori, T. 1965. On the tsunami which accompanied the Niigata earthquake of June 16, 1964. *Bull. Earthquake Res. Inst. Tokyo Univ.* 43:129–48
13. Hatori, T. 1966. Vertical displacement in a tsunami source area and the topography of the sea bottom. *Bull. Earthquake Res. Inst. Tokyo Univ.* 44:1449–64
14. Hatori, T. 1967. The generating area of Sanriku tsunami of 1896 and its comparison with the tsunami of 1933. *J. Seismol. Soc. Jap.* 20:164–70 (in Japanese)
15. Hirasawa, T. 1965. Source mechanism of the Niigata earthquake of June 16, 1964, as derived from body waves. *J. Phys. Earth* 13:35–66
16. Honda, H. 1932. On the mechanism and the types of the seismograms of shallow earthquakes. *Geophys. Mag.* 5:69–88
17. Ichikawa, M. 1971. Reanalyses of mechanism of earthquakes which occurred in and near Japan, and statistical studies on the nodal plane solutions obtained, 1926–1968. *Geophys. Mag.* 35:207–74
18. Imamura, A. 1928. On the destructive

Annu. Rev. Earth. Planet. Sci. 1973.1:213-239. Downloaded from arjournals.annualreviews.org
by CALIFORNIA INSTITUTE OF TECHNOLOGY on 09/13/05. For personal use only.

Annual Reviews
www.annualreviews.org/aronline

Tango earthquake of March 7, 1927. *Bull. Earthquake Res. Inst. Tokyo Univ.* 4:179–202 (in Japanese)
19. Imamura, A. 1930. Topographical changes accompanying earthquakes or volcanic eruptions. *Publ. Earthquake Invest. Comm. Foreign Lang.* 25:1–143
20. Imamura, A. 1931. Seismometric study of the recent destructive N. Idu earthquake. *Bull. Earthquake Res. Inst. Tokyo Univ.* 9:36–49 (in Japanese)
21. Imamura, A. 1937. *Theoretical and Applied Seismology.* Tokyo: Maruzen. 358 pp.
22. Kanamori, H. 1971. Faulting of the great Kanto earthquake of 1923 as revealed by seismological data. *Bull. Earthquake Res. Inst. Tokyo Univ.* 49:13–18
23. Kanamori, H. 1971. Great earthquakes at island arcs and the lithosphere. *Tectonophysics* 12:187–98
24. Kanamori, H. 1972. Relations between tectonic stress, great earthquake and earthquake swarm. *Tectonophysics* 14: 1–12
25. Kanamori, H. 1972. Tectonic implications of the 1944 Tonankai and the 1946 Nankaido earthquakes. *Phys. Earth Planet. Interiors* 5:129–39
26. Kanamori, H. 1972. Determination of effective tectonic stress associated with earthquake faulting—Tottori earthquake of 1943. *Phys. Earth Planet. Interiors.* 5:426–34
27. Kanamori, H. 1972. Mechanism of tsunami earthquakes. *Phys. Earth Planet. Interiors.* Vol. 5. In press
28. Kanamori, H., Abe, K. 1968. Deep structure of island arcs as revealed by surface waves. *Bull. Earthquake Res. Inst. Tokyo Univ.* 46:1001–25
29. Kasahara, K. 1957. The nature of seismic origins as inferred from seismological and geodetic observations, 1. *Bull. Earthquake Res. Inst. Tokyo Univ.* 35:473–532
30. Kasahara, K. 1972. Earthquake fault studies in Japan. *Trans. Roy. Soc.* In press
31. Kayano, I. 1968. Determination of origin times, epicenters and focal depths of aftershocks of the Niigata earthquake of June 16, 1964. *Bull. Earthquake Res. Inst. Tokyo Univ.* 46:223–69
32. Knopoff, L. 1958. Energy release in earthquakes. *Geophys. J.* 1:44–52
33. Komura, S. 1958. A consideration about the mechanism of occurrence of large-scale earthquakes. *Mem. Coll. Sci. Univ. Kyoto Ser. A.* 28:363–89
34. Land Survey Department. 1930. *Result Revision 3rd order Triangulations Tango Dist., Land Surv. Dep., Tokyo.* 8 pp.
35. Matsuda, T. 1968. Active faults and active folding. *Symp. Res. Earthquake Predict., Tokyo,* 46–49 (in Japanese)
36. Matuzawa, T. 1964. *Study of Earthquakes.* Tokyo: Uno Shoten. 213 pp.
37. Miyabe, N. 1934. On the vertical earth movement in Kwanto districts. *Bull. Earthquake Res. Inst. Tokyo Univ.* 9:1–21
38. Miyabe, N. 1955. Vertical earth movement in Nankai district. *Bull. Geogr. Surv. Inst.* 4:1–14
39. Miyamura, S. 1962. Types of crustal movements accompanied with earthquakes. *Proc. 1st Int. Symp. Recent Crustal Movements, Leipzig,* 235–51
40. Mogi, A. 1959. On the depth change at the time of Kanto earthquake in Sagami Bay. *Hydrogr. Bull.* 60:52–60 (in Japanese)
41. Mogi, A., Kawamura, B., Iwabuchi, Y. 1964. Submarine coastal movement due to the Niigata earthquake of 1964, in the environs of the Awa Sima island, Japan Sea. *J. Geodetic Soc. Jap.* 10:180–86
42. Mogi, K. 1963. Some discussions of aftershocks, foreshocks and earthquake swarms. *Bull. Earthquake Res. Inst. Tokyo Univ.* 41:615–58
43. Mogi, K. 1968. Development of aftershock areas of great earthquakes. *Bull. Earthquake Res. Inst. Tokyo Univ.* 46: 175–203
44. Muto, K. 1932. A study of displacements of triangulation points. *Bull. Earthquake Res. Inst. Tokyo Univ.* 10: 384–92
45. Muto, K., Okuda, T., Harada, Y. 1950. The land deformation accompanying the Fukui earthquake of June 28, 1948. *Bull. Geogr. Surv. Inst.* 2:27–36
46. Nakamura, K. 1971. Volcano as a possible indicator of crustal strain. *Bull. Volcanol. Soc. Jap.* 16:63–71
47. Nakamura, K., Kasahara, K., Matsuda, T. 1964. Tilting and uplift of an island, Awashima, near the epicenter of the Niigata earthquake in 1964. *J. Geodetic Soc. Jap.* 10:172–86
48. Nasu, N. 1935. Supplementary study on the stereometrical distribution of the aftershocks of the great Tango earthquake of 1927. *Bull. Earthquake Res. Inst. Tokyo Univ.* 13:325–99
49. Nasu, N. 1950. Crustal deformation. In *The Fukui Earthquake of June 28, 1948,* ed. H. Tsuya, 93–130. Tokyo: Committee for the Study of Fukui Earthquake. 197 pp.
50. Nishimura, E. 1962. Anomalous tilting

Annu. Rev. Earth. Planet. Sci. 1973.1:213-239. Downloaded from arjournals.annualreviews.org
by CALIFORNIA INSTITUTE OF TECHNOLOGY on 09/13/05. For personal use only.

Annual Reviews
www.annualreviews.org/aronline

movement of the ground observed before destructive earthquakes. *Proc. 1st Int. Symp. Recent Crustal Movements, Leipzig,* 214–34
51. Ogawa, M. 1949. Seismic vibrations of the Fukui earthquake observed at the Abuyama Seismological Observatory. *Bull. Disaster Prev. Res. Inst. Kyoto Univ.* 2:122–23
52. Okada, A., Nagata, T. 1953. Land deformation of the neighborhood of Muroto point after the Nankaido great earthquake in 1946. *Bull. Earthquake Res. Inst. Tokyo Univ.* 31:169–77
53. Okuda, T. 1950. On the mode of the vertical land-deformation accompanying the great Nankaido earthquake 1946. *Bull. Geogr. Surv. Inst.* 2:37–59
54. Omote, S. 1950. Aftershocks. In *The Fukui Earthquake of June 28, 1948,* ed. H. Tsuya, 37–78. Tokyo: Committee for the Study of Fukui Earthquake, 197 pp.
55. Omote, S. 1955. Aftershocks that accompanied the Tottori earthquake of Sept. 10, 1943, 2. *Bull. Earthquake Res. Inst. Tokyo Univ.* 33:641–61
56. Richter, C. F. 1958. *Elementary Seismology.* San Francisco: W. H. Freeman. 768 pp.
57. Sato, Y., Nakane, K. 1972. Faulting associated with Tottori earthquake. *Bull. Geogr. Surv. Inst. Jap.* 17. In press
58. Smith, S. W., Wyss, M. 1968. Displacement on the San Andreas fault initiated by the 1966 Parkfield earthquake. *Bull. Seismol. Soc. Am.* 58:1955–74
59. Sugimura, A. 1967. Uniform rates and duration period of Quaternary earth movements in Japan. *J. Geosci. Osaka City Univ.* 10:25–35
60. Sugimura, A., Naruse, Y. 1954. Changes in sea level, seismic upheavals, and coastal terraces in the southern Kanto region, 1. *Jap. J. Geol. Geogr.* 24:101–13
61. Sugimura, A., Naruse, Y. 1955. Changes in sea level, seismic upheavals, and coastal terraces in the southern Kanto region, 2. *Jap. J. Geol. Geogr.* 26:165–76
62. Tazima, M., Fujita, N., Sato, Y. 1970. Mode of the recent crustal deformation in Japan. *Proc. Symp. Thermal Structure Beneath the Japanese Islands,* 117–32 (in Japanese)
63. Tsuboi, C. 1932. Investigation on the deformation of the earth's crust in the Tango district connected with the Tango earthquake of 1927 (Part 4). *Bull. Earthquake Res. Inst. Tokyo Univ.* 10:411–34
64. Tsuboi, C. 1933. Investigation on the deformation of the earth's crust found by precise geodetic means. *Jap. J. Astron. Geophys.* 10:93–248
65. Tsubokawa, I. 1969. On relation between duration of crustal movement and magnitude of earthquake expected. *J. Geodetic Soc. Jap.* 15:75–88 (in Japanese)
66. Tsuya, H. 1944. The Shikano and Yoshioka faults and geology of the region affected by the Tottori earthquake of 1943. *Bull. Earthquake Res. Inst. Tokyo Univ.* 22:1–32 (in Japanese)
67. Utsu, T. 1957. Magnitude of earthquake and occurrence of their aftershocks. *J. Seismol. Soc. Jap.* 10:35–54 (in Japanese)
68. Watanabe, A. 1929. Preliminary note on the coastal terraces of the southern parts of Boso peninsula. *Geogr. Rev. Jap.* 5:119–26 (in Japanese)
69. Watanabe, A. 1932. The geomorphology of the coastal district of southeastern Shikoku. *Bull. Earthquake Res. Inst. Tokyo Univ.* 10:209–34
70. Yamasaki, N., Tada, F. 1928. The Oku-Tango earthquake of 1927. *Bull. Earthquake Res. Inst. Tokyo Univ.* 4:159–77
71. Yonekura, N. 1972. A review on seismic crustal deformations in and near Japan. *Bull. Dep. Geogr. Univ. Tokyo* 4:17–50
72. Yoshikawa, T. 1970. On the relations between Quaternary tectonic movement and seismic crustal deformation in Japan. *Bull. Dep. Geogr. Univ. Tokyo* 2:1–24
73. Yoshikawa, T., Kaizuka, S., Ôta, Y. 1964. Crustal movement in the late Quaternary revealed with coastal terraces on the southeast coast of Shikoku, southwestern Japan. *J. Geodetic Soc. Jap.* 10:116–22

Annu. Rev. Earth. Planet. Sci. 1973.1:213-239. Downloaded from arjournals.annualreviews.org
by CALIFORNIA INSTITUTE OF TECHNOLOGY on 09/13/05. For personal use only.

CONTENTS

Annu. Rev. Earth. Planet. Sci. 1973.1:213-239. Downloaded from arjournals.annualreviews.org
by CALIFORNIA INSTITUTE OF TECHNOLOGY on 09/13/05. For personal use only.